

---

# Confocal Examination of Nonmelanoma Cancers in Thick Skin Excisions to Potentially Guide Mohs Micrographic Surgery Without Frozen Histopathology

Milind Rajadhyaksha,\*† Gregg Menaker,† Thomas Flotte,† Peter J. Dwyer,\* and Salvador González†

\*Lucid Inc, Rochester, New York, New York, U.S.A.; †Wellman Laboratories-Dermatology Service, Massachusetts General Hospital, Harvard Medical School, Boston, Massachusetts, U.S.A.

---

**Precise removal of nonmelanoma cancers with minimum damage to the surrounding normal skin is guided by the histopathologic examination of each excision during Mohs micrographic surgery. The preparation of frozen histopathology sections typically requires 20–45 min per excision. Real-time confocal reflectance microscopy offers an imaging method potentially to avoid frozen histopathology and prepare noninvasive (optical) sections within 5 min. Skin excisions ( $\approx 1$  mm thick) from Mohs surgeries were washed with 5% acetic acid and imaged with a confocal cross-polarized microscope. The confocal images were compared with the corresponding histopathology. Acetic acid causes compaction of chromatin that increases light back-scatter and makes the nuclei bright and easily detectable. Crossed-polarization strongly enhances the contrast**

**of the nuclei because the compacted chromatin depolarizes the illumination light whereas the surrounding cytoplasm and normal dermis does not. Fast low-resolution examination of cancer lobules in wide fields of view followed by high-resolution inspection of nuclear morphology in small fields of view is possible; this is similar to the procedure for examining histopathology sections. Both the Mohs surgeon and the patient will potentially save several hours per day in the operating room. Fast confocal reflectance microscopic examination of excisions (of any thickness) may improve the management of surgical pathology and guide microsurgery of any human tissue. Key words: dermatology/lasers/optical imaging/optical microscopy/scanning/surgical pathology. *J Invest Dermatol* 117:1137–1143, 2001**

---

**T**he removal of epithelial cancers in high-risk anatomical sites requires precise microsurgical excision with minimum damage to the surrounding normal tissue, and is guided by the histopathologic examination of each excision during the surgery. A well known example is Mohs micrographic surgery for excision of nonmelanoma skin cancers (Mohs, 1941; Mikhail, 1991). Non-melanoma skin cancers include basal cell carcinoma (BCC) and squamous cell carcinoma (SCC) that occur today at a rate of more than 1 million new cases every year (Marwick, 1995). These cancers have a high morbidity, occurring most frequently on the faces of people over 40. Because the cancers occur in high-risk areas such as on or near the nose, eyes, ears, or mouth, precise microsurgical excision must be performed to remove only the cancer and leave the surrounding normal skin as intact as possible.

A Mohs procedure requires two excisions, in general, and several, in many cases of large complex lesions. The excisions are typically 1 mm thick and 2–20 mm in extent. Frozen, hematoxylin and eosin (H&E)-stained, horizontal (*en face*) sections are prepared; this requires 20–45 min for each excision during which the patient has to wait with an open wound under local anesthesia. Thus, a Mohs procedure typically lasts from one to several hours. This is

slow and time inefficient for Mohs surgeons, most of whom perform several procedures per day. We may avoid the preparation of frozen histopathology sections, significantly save time for the patient and make Mohs micrographic surgery much faster by the use of confocal reflectance microscopy to examine the thick skin excisions in noninvasive (optical) sections.

Confocal reflectance microscopy is an optical method that noninvasively images nuclear and cellular morphology in 2–5  $\mu\text{m}$  thin sections in living human skin with lateral resolution of 0.5–1.0  $\mu\text{m}$  (New *et al*, 1991; Corcuff and Leveque, 1993; Corcuff *et al*, 1993, 1996; Bertrand and Corcuff, 1994; Kaufman *et al*, 1995; Masters *et al*, 1997a,b; Rajadhyaksha *et al*, 1995, 1999a). The confocal (optical) section thickness compares very well to the typically 5  $\mu\text{m}$  thin sections that are prepared for conventional (frozen or fixed) histopathology. Skin can be imaged either *in vivo* or *ex vivo* (freshly excised, thick specimens) without any processing. Thus, confocal imaging of nonmelanoma skin cancers during Mohs procedures is possible without conventional histopathology. Fast examination of the cancers within the 1 mm thick skin excisions may be achieved within minutes, with the use of contrast agents to enhance the detection of the cancers. To enhance the contrast of the nuclei within the BCC and SCC, we use 5% acetic acid. Acetic acid causes whitening of epithelial tissue (Burghardt, 1959) and, at 45% concentration, compaction of chromatin within nuclei due to extraction of histone proteins (Fraschini *et al*, 1981). In confocal brightfield images, acetic acid makes the nuclei appear bright instead of dark (Smithpeter *et al*, 1998; Drezek *et al*, 2000).

---

Manuscript received December 8, 2001; revised May 17, 2001; accepted for publication June 11, 2001.

Reprint requests to: Dr. Milind Rajadhyaksha, Dermatology—Bartlett Extension 630, Massachusetts General Hospital, Boston, MA 02114. Email: rajadmil@helix.mgh.harvard.edu

In this study, we describe the use of 5% acetic acid and confocal cross-polarized microscopy to enhance the contrast of the nuclei and examine BCC and SCC in thick skin excisions from Mohs micrographic surgery. Confocal images of the compaction of chromatin caused by acetic acid and the corresponding histology are shown. The optical back-scattering mechanism is explained, by which compacted chromatin causes brightening of the nuclei as well as depolarization of the illumination light that subsequently leads to contrast enhancement of the cancers. Comparison of confocal images of the cancers to the corresponding histopathology is shown. Optimum imaging parameters are presented that are relevant for clinical use.

## MATERIALS AND METHODS

**Excised tissue preparation** Skin excisions (typically 1 mm thick) from Mohs micrographic surgeries were obtained from the Dermatologic Surgery Unit at Massachusetts General Hospital under an IRB-approved protocol. The skin that remained (and is otherwise discarded) was collected after the Mohs histotechnician had taken the first few sections; thus, the experiments did not interfere with the routine Mohs surgical procedures and patient care. The skin excisions were frozen when the histotechnician had prepared the sections. The fresh-frozen skin was thawed, rinsed with Dulbecco's phosphate-buffered solution, washed with 5% acetic acid for 30 s, and then imaged with the confocal microscope. The control images were of skin that was thawed and rinsed in Dulbecco's phosphate-buffered solution but not washed with acetic acid.

**Confocal imaging** Two confocal microscopes were used: our original video-rate (30 frames per s) laboratory prototype and its commercial version (VivaScope 2000, Lucid, Rochester, NY). The instrumentation and imaging details have been previously reported; the illumination is at the near-infrared wavelength of 1064 nm, water immersion objective lenses are used, and detector aperture (pinhole) diameters are 1–10 resels, where 1 resel is equal to the lateral resolution (Rajadhyaksha *et al*, 1995, 1999a,b). The illumination laser beam is linearly polarized perpendicular (p-state) to the plane of incidence (i.e., parallel to the tissue surface). A linear polarizer (analyzer) is placed in front of the detector and oriented such that, when its transmission axis is parallel to the illumination p-state, brightfield (parallel-polarized) images are obtained. When the transmission axis of the detection analyzer is oriented perpendicular to the illumination p-state, the images are cross-polarized.

The following objective lenses (with experimentally measured section thickness) were used: (i) 20 $\times$ /0.3 NA or 10 $\times$ /0.3 NA (section thickness  $\approx$ 30  $\mu$ m) for low-resolution examination of suspected cancerous sites in wide fields of view of 1–2 mm; (ii) 60 $\times$ /0.9 NA or 30 $\times$ /0.9 NA (section thickness  $\approx$ 3  $\mu$ m) for high resolution inspection of nuclear morphology in small fields of view of 0.25–0.50 mm; and (iii) 100 $\times$ /1.2 NA (section thickness  $\approx$ 2  $\mu$ m) for very high resolution imaging of the effects of acetic acid on chromatin in a small field of view of 0.15 mm. The maximum field of view (1–2 mm) of the confocal microscope is much smaller than most excisions. To examine the entire excision, a sequence of images of adjacent fields was digitally captured in a two-dimensional matrix, while translating the excision on an automated two-dimensional stage. These images were at low resolution in a wide field of view, obtained with either the 20 $\times$ /0.3 NA or the 10 $\times$ /0.3 NA objective lens. The images were stitched together using commercially available software (IPLab Spectrum, version 3.1, Scanalytics, Vienna, VA) to create a mosaic that showed the entire excision. The mosaic is essentially a low-resolution map showing the location, shape, and general morphology of the BCC or SCC within the excision. Within a mosaic, we first identify the fields that contain bright patterns that are suspected to be of acetic acid-washed nuclei; those fields are then imaged at high resolution, with either the 30 $\times$ /0.9 NA or 60 $\times$ /0.9 NA objective lens, to inspect further the morphology of the bright patterns. Images obtained in brightfield (parallel polarization) were compared with those with crossed polarization.

**Histopathology** The excisions that were confocally imaged for the effects of 5% acetic acid on chromatin were cut into 1 mm cubes and fixed in glutaraldehyde/paraformaldehyde. The tissue was then processed for Epon plastic embedding. The blocks were cut into 1  $\mu$ m sections and stained with toluidine blue. As a control, we prepared histology sections of skin that was not washed with acetic acid.

The excisions that were confocally examined for BCC and SCC were fixed in 10% formalin, and processed for routine H&E-stained histo-

pathology. Horizontal or *en face* sections were prepared, similar to those cut by the Mohs histotechnician. To assess the effect of 5% acetic acid on permanent histopathology, H&E sections of acetic acid-washed excisions were compared with those of control skin from the same patient. The confocal images and mosaics were compared with the histopathology sections for the location, shape, general appearance, and nuclear morphology of the cancers.

To estimate the potential saving in time when using confocal reflectance microscopy, the time required to prepare frozen histopathology sections was measured with a stop watch for a wide range of skin excisions during Mohs surgeries in two clinics, including that of one co-author (GM). This was compared with the time required to prepare confocal mosaics.

## RESULTS

**Nuclei in basal and squamous cells lack contrast relative to the dermis in confocal brightfield images (Fig 1)** When basal and squamous cells from the epidermis invade the underlying dermis (as in BCC and SCC), examination of the cancer is difficult in confocal brightfield images because the nuclei lack contrast relative to the surrounding cytoplasm and collagen (Fig 1). The dark nuclei and bright cells (Fig 1a) are not easily seen within the bright-and-dark matrix of collagen (Fig 1b).

**Washing 1 mm thick excised human skin with 5% acetic acid for 30 s causes the nuclei to appear bright (Fig 2) due to the compaction of chromatin (Fig 3)** A brightening of the epidermis is observed at low resolution (Fig 2a), caused by the individual nuclei becoming bright, as seen at high resolution (Fig 2b). In confocal images of human epidermis, the thin and diffuse chromatin filaments are not detected and the nuclei

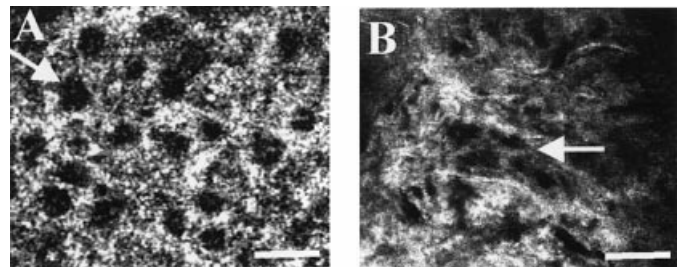


**Figure 1. In confocal brightfield images, examination of BCC and SCC in the dermis is difficult because the nuclei lack contrast relative to the surrounding cytoplasm and collagen.** The nuclei appear as dark ovals (a, arrow) and the cytoplasm appears bright in squamous and basal cells in the epidermis. The collagen in the underlying dermis appears as bright fibers or bundles with dark spaces in between (b, arrow). These dark spaces appear similar to atypical nuclei of irregular shapes and sizes, as in the BCC and SCC. Objective lens 60 $\times$ /0.9 NA, scale bar: 25  $\mu$ m.

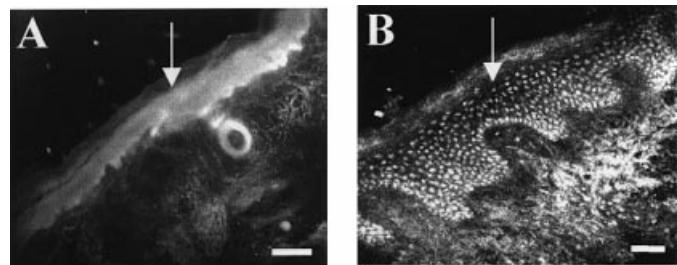


**Figure 2. Confocal brightfield images of excised skin, after washing with 5% acetic acid for thirty seconds show brightened epidermis.** At low resolution the individual nuclei are not resolved (a, arrow). Objective lens 20 $\times$ /0.3 NA, scale bar: 100  $\mu$ m; individual bright nuclei (b, arrow) in the epidermis are seen at high resolution. Objective lens 60 $\times$ /0.9 NA, scale bar: 25  $\mu$ m.

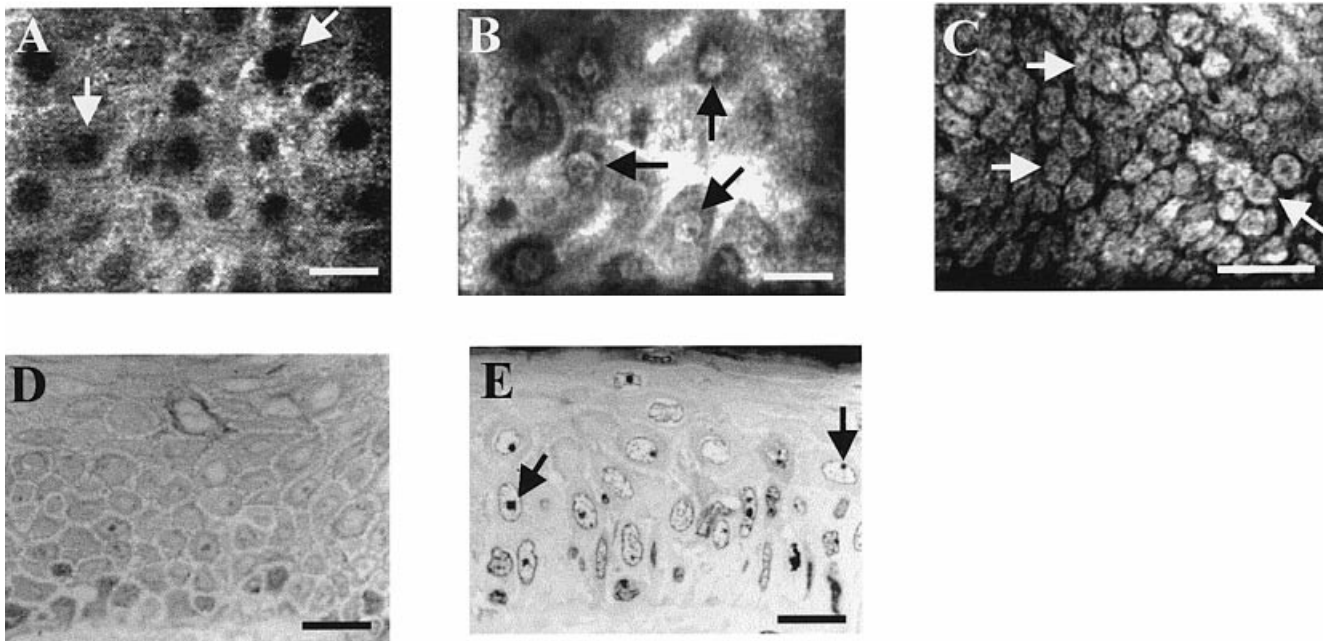


**Figure 3. Washing excised skin with 5% acetic acid for 30 s causes compaction of chromatin.** In human epidermis, the very thin and diffuse chromatin is not detected and hence the nuclei always appear dark (*a*, arrows). The compacted chromatin, due to acetic acid, is of large size (1–5  $\mu\text{m}$ ) and fills the intranuclear volume (*b,c*, arrows). The nuclei appear bright in the confocal images of both normal skin (*b*, arrows) and BCC (*c*, arrows). The confocal observations (in horizontal sections) correlate well to that in the corresponding histology (shown in standard vertical sections): no compaction in normal skin (*d*) but clearly seen after washing with acetic acid (*e*, arrows) in glutaraldehyde/paraformaldehyde-fixed, plastic-embedded, toluidine blue-stained sections. Objective lens 100  $\times$ /1.2 NA, scale bar: 25  $\mu\text{m}$ .

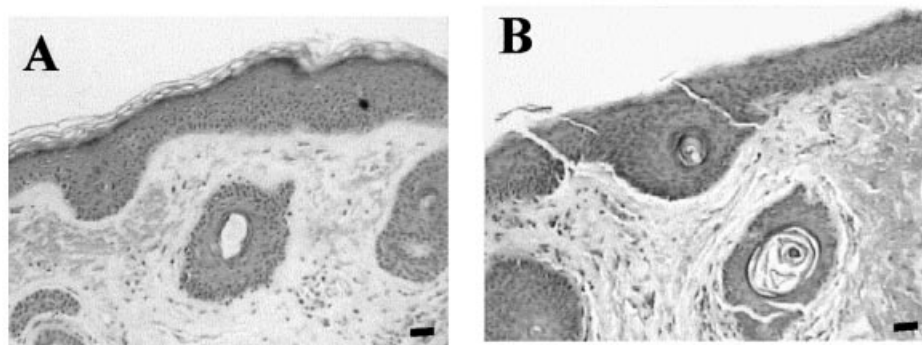


**Figure 4. Permanent histopathology is not affected by 5% acetic acid-washing.** In paraffin-embedded H&E sections, no differences in the nuclear morphology, cytoplasmic staining, and extracellular matrix are seen between control skin (*a*) and acetic acid-washed skin (*b*). Objective lens 10  $\times$ /0.25 NA; scale bar: 25  $\mu\text{m}$ .

normally appear dark (**Fig 3a**); however, the acetic acid induced compacted chromatin is of large size (1–5  $\mu\text{m}$ ), substantially fills the intranuclear volume and is easily detected; the nuclei then appear bright in confocal images of both normal skin (**Fig 3b**) and cancerous skin (**Fig 3c**). As in the confocal images, the compaction of the chromatin is not seen in the corresponding histology of normal skin (**Fig 3d**) but clearly seen after washing with acetic acid (**Fig 3e**). There is peripheral condensation as well as clumping of the chromatin.

**Permanent histopathology is not affected by 5% acetic acid washing (Fig 4)** Examination of H&E sections showed that there are no differences in the nuclear morphology, cytoplasmic staining, and extracellular matrix between control skin (**Fig 4a**) and acetic acid-washed skin (**Fig 4b**). **Figure 4** does not show the acetic acid-induced compaction of chromatin that is clearly seen in **Fig 3**, most probably because of the differences in tissue processing; this is further explained in the *Discussion*.

**The contrast in the confocal cross-polarized images is significantly better than that in the brightfield (parallel-polarized) images (Fig 5)** In brightfield images, the examination of the acetic acid-induced bright nuclei, when they invade the underlying collagen (as in BCC and SCC), is, unfortunately, still difficult because there are now bright nuclei appearing on a background of bright cytoplasm and collagen. There is, again, a lack of contrast, as can be inferred from **Fig 2b**. To suppress the brightness of the cytoplasm and dermis, the images are obtained in crossed polarization instead of brightfield.

In real-time confocal images observed through a rotating analyzer, the brightness of the nuclei does not vary much, but the brightness of the cytoplasm and dermis varies from maximum to minimum (dark). The acetic acid-washed nuclei significantly depolarize the linearly polarized illumination light; however, the detected light from the surrounding cytoplasm and normal dermis maintains its linear polarization. Thus, in the brightfield images, the cytoplasm and dermis are bright such that the cancer appears with

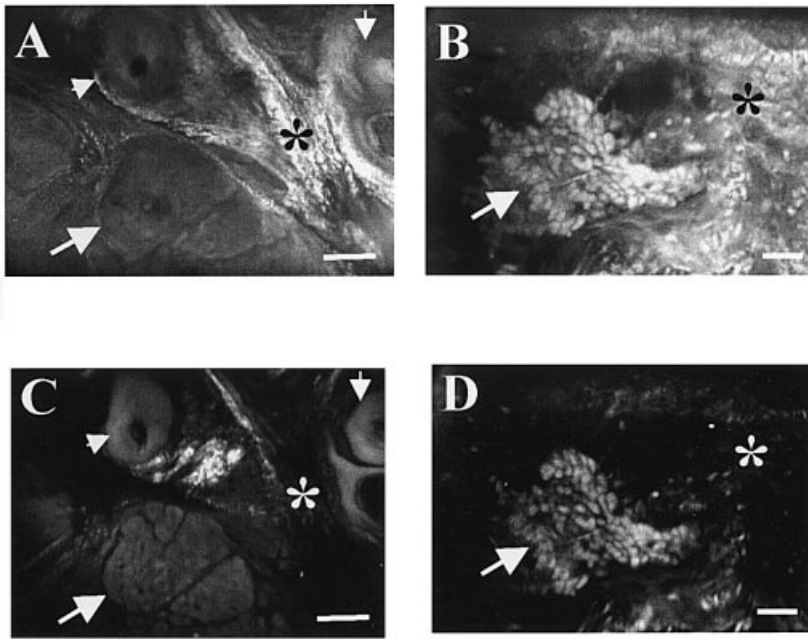


**Figure 5. Compared with confocal brightfield (parallel-polarized) images, the contrast is significantly better in the cross-polarized images.** This happens because the acetic acid-washed nuclei significantly depolarize the linearly polarized illumination light whereas the surrounding cytoplasm and dermis does not. In the brightfield images, the surrounding dermis is bright (\* in *a, b*) and the BCC appears at low contrast: both the general morphology at low resolution in a wide field-of-view (*a, arrow*) and nuclear morphology at high resolution in a small field-of-view (*b, arrow*) are poorly visualized. Hair follicles (*a, arrowheads*) often cannot be distinguished from the cancer (*a, arrow*). In cross-polarized images, the dermis is dark (\* in *c, d*). The general morphology of the BCC (*c, arrow*) and nuclear morphology (*d, arrow*) is better visualized at high contrast. The surrounding hair follicles (*c, arrowheads*) are well distinguished from the cancer (*c, arrow*). The crossed polarization darkens the dermis significantly but not completely, and consequently, bright or gray areas within the dermis are seen near the hair follicle and BCC in the upper central portion of image (*d*). Objective lenses  $20\times/0.3$  NA (*a, c*),  $60\times/0.9$  NA (*b, d*), scale bar:  $100\ \mu\text{m}$  (*a, c*),  $25\ \mu\text{m}$  (*b, d*).

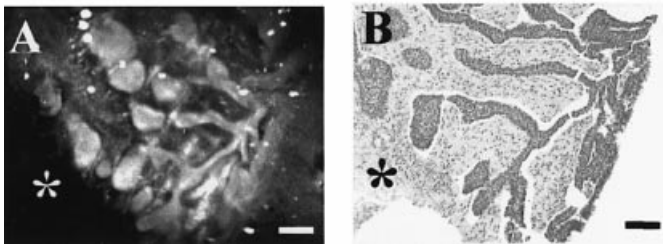


**Figure 6. Low resolution (0.3 NA, section thickness  $\approx 30\ \mu\text{m}$ ) confocal cross-polarized image of an acetic acid-washed BCC correlates well to the corresponding histopathology.** In the confocal image, the BCC appears bright whereas the surrounding collagen (\* in *a*) appears dark; in the histopathology, this corresponds to the dark-stained BCC (actually, purple-stained in color) within lightly stained collagen (actually, pink-stained in color) (\* in *b*). The general morphology, shape, and size of individual cancer lobules is clearly delineated, similar to that seen in the histopathology. Objective lenses  $20\times/0.3$  NA (*a*),  $6.3\times/0.2$  NA (*b*); scale bar:  $100\ \mu\text{m}$ .

low contrast (Fig 5*a,b*). In the cross-polarized images, however, the cytoplasm and dermis are dark and the cancer appears with enhanced contrast (Figs 5*c,d*). Consequently, we can clearly examine both the general morphology (Fig 5*e*) as well as the nuclear morphology (Fig 5*d*). The crossed polarization darkens the dermis significantly but not completely, and consequently, bright or gray areas are seen within the dermis.

#### Confocal images of acetic acid-washed cancers correlate well with the corresponding histopathology (Figs 6 and 7)

In confocal cross-polarized images of a BCC at low resolution (0.3 NA, section thickness  $\approx 30\ \mu\text{m}$ ), the general morphology of the BCC appears bright, whereas the surrounding collagen appears dark (Fig 6*a*). The location, shape, and size of the cancer is clearly delineated. This compares well with the morphology seen in the corresponding histopathology (Fig 6*b*). At high resolution (0.9 NA, section thickness  $\approx 3\ \mu\text{m}$ ), the atypical morphology of individual nuclei is clearly seen (Fig 7*a*). The nuclei appear pleomorphic (i.e., of varying shapes and sizes), crowded (i.e., increased density), are distributed in a disorderly pattern and exhibit

peripheral palisading. Again, this compares well with the corresponding histopathology (Fig 7*b*).

**Confocal mosaics allow fast low-resolution examination of cancer in large skin excisions (Fig 8)** Good correlation is observed between the confocal mosaic of a BCC (Fig 8*a*) and the corresponding histopathology (Fig 8*b*) in terms of location, shape, size, and general morphology. At low resolution, the cancer lobules are easily delineated from the surrounding normal dermis and adnexal structures. At high resolution, individual nuclei are accurately visualized allowing distinction between cancerous and normal healthy cells. With the automated stage translation and image digitizing routine, a mosaic of  $10\times 10$  mm area of tissue can be created in 3.5 min. Table I demonstrates the potential saving in time when examining excisions during Mohs surgery using confocal reflectance microscopy.

## DISCUSSION

#### Washing 1 mm thick excised skin with 5% acetic acid makes the nuclei appear bright

Normally, the nuclei appear dark as seen here (Fig 3*a*) and in all other confocal imaging studies of normal and pathologic human skin (New *et al*, 1991; Corcuff and Leveque, 1993; Corcuff *et al*, 1993, 1996; Bertrand and Corcuff, 1994; Kaufman *et al*, 1995; Masters *et al*, 1997*a,b*; Rajadhyaksha *et al*, 1995, 1999*a*). This is because of minimal back-scatter from the very thin (30–100 nm), diffuse chromatin that normally occupies a very small volume within the nucleus (Fawcett, 1986; Alberts *et al*, 1989). Acetic acid makes the nuclei bright due to significant back-scatter from the compacted chromatin, which is of large size (1–5  $\mu\text{m}$ ) and fills the intranuclear volume (Fig 3*b,c*).

The appearance of nuclei as bright or dark may be understood from an approximate analysis<sup>1</sup> of detected signals (i.e., back-scattered light) using Mie optical scattering theory (van de Hulst, 1981). We assume: (i) illumination of 10 mW at the near infrared wavelength of 1064 nm; (ii) video-rate (30 frames per s) imaging with an objective lens of 0.9 NA; (iii) refractive indices of the nucleus and surrounding cytoplasm to be 1.39 (Brunsting and

<sup>1</sup>Rajadhyaksha M, Henrichs M, Ananth KP, Chang HT, Gonzalez S: Reflectance and fluorescent contrast agents for real-time *in vivo* confocal imaging. *Opt Soc Am Biomed Topical Meet Tech Digest* 182–184, 2000 (Abstr.)

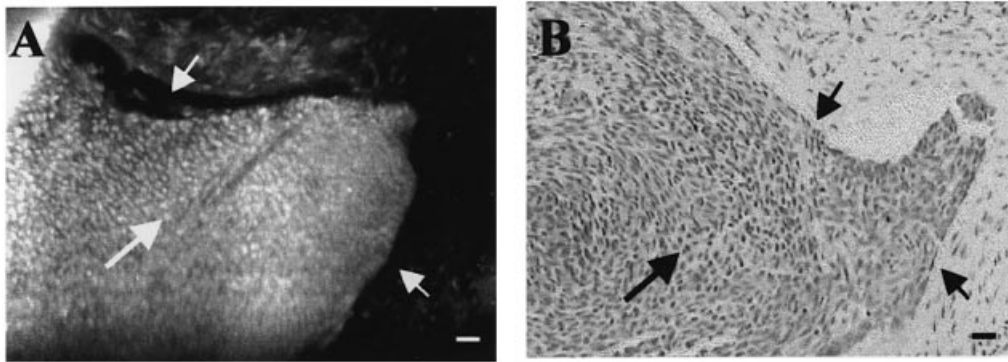


**Figure 7. High resolution (0.9 NA, section thickness  $\approx 3 \mu\text{m}$ ) confocal cross-polarized image of an acetic acid-washed BCC showing clearly the atypical morphology of individual nuclei.** The nuclei appear bright in the confocal image (*a*, arrow) and these correspond to the dark-stained (actually, purple-stained in color) nuclei in the histopathology (*b*, arrow). The nuclei appear pleomorphic (i.e., of varying shapes and sizes), crowded (i.e., increased density), are distributed in a disorderly pattern and exhibit peripheral palisading. The increased cellularity of the cancer compared with the surrounding dermis is well visualized. A cleft surrounding the BCC is seen in the confocal image (*a*, arrowheads) similar to that seen in the corresponding histopathology (*b*, arrowheads). Objective lenses  $30\times/0.9$  NA (*a*),  $10\times/0.25$  NA (*b*); scale bar:  $25 \mu\text{m}$ .

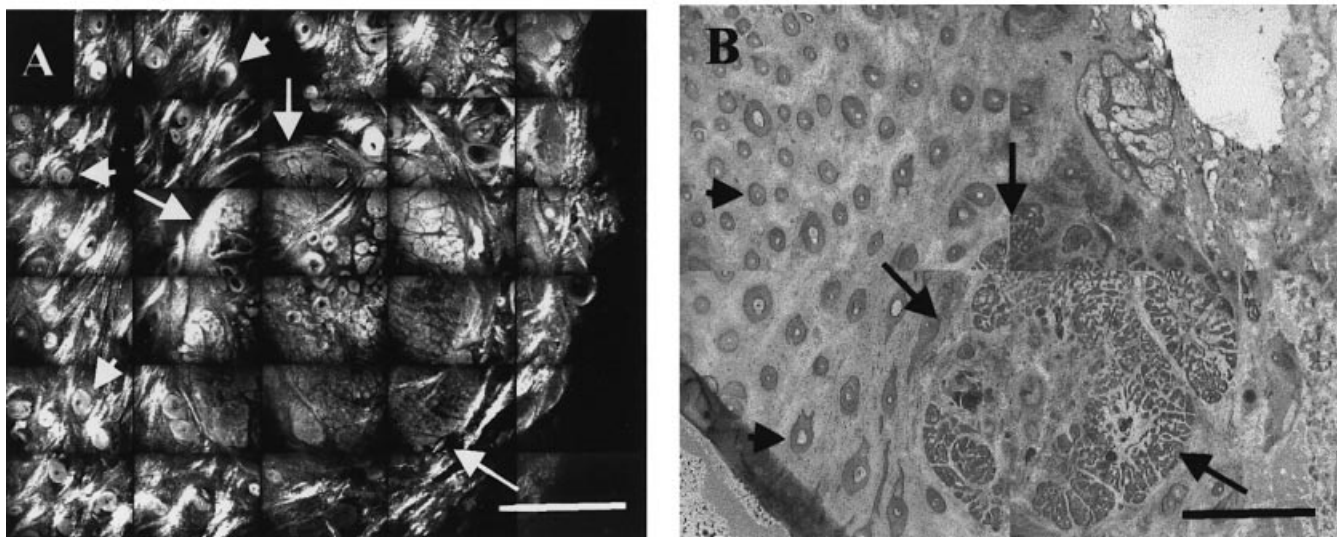


**Figure 8. Confocal mosaics allow fast low-resolution examination of cancer in large excisions.** The confocal mosaic of a BCC (*a*, arrows) compares well to the corresponding histopathology (*b*, arrows) in terms of location, shape, size, and general morphology. Hair follicles are seen in both images (*a,b*, arrowheads). Objective lens  $20\times/0.3$  NA (*a*),  $2.5\times/0.07$  NA (*b*); scale bar = 1 mm.

**Table I. Potential saving in time when examining acetic acid-washed skin excisions during Mohs surgery with confocal cross-polarized imaging<sup>a</sup>**

Preparation of frozen histopathology sections	Preparation of confocal mosaics
Freezing skin excision, embedding and sectioning: 9–30 min	Washing skin excision with acetic acid: 0.5 min
H&E staining: 12 min	Mounting on confocal microscope: 1 min
Mounting on slide with coverslip: 1 min	Creating a mosaic: 3.5 min for $10\times 10$ mm (achieved), 5 min for $20\times 20$ mm (expected)
Total time: 22–43 min	Total time: 5–6.5 min

<sup>a</sup>Comparison of the times required to prepare frozen histopathology sections vs confocal mosaics.

Mullaney, 1974) and 1.34 (Tearney *et al*, 1995), respectively; and (iv) the nuclei to be at a depth of either  $25 \mu\text{m}$  (granular layer) or

$50 \mu\text{m}$  (spinous layer) in human epidermis. For chromatin filaments of size  $100 \text{ nm}$ , the detected signal is calculated to be  $\approx 150\text{--}500$  photons per pixel at depths of  $50\text{--}25 \mu\text{m}$ . This is a weak signal that is within the background noise and not detected with a confocal reflectance microscope. Therefore, the nuclei appear dark (Fig 3a). By comparison, for compacted chromatin of size  $1 \mu\text{m}$ , the detected signal is  $\approx 2\text{--}7 \times 10^4$  photons per pixel at depths of  $50\text{--}25 \mu\text{m}$ . This is a strong signal and thus the nuclei appear bright (Figs 3b,c).

Near-infrared ( $1064 \text{ nm}$ ) illumination with an Nd:YAG laser was used because the confocal microscope is set up to image skin *in vivo* as deep as possible; however, when examining nonmelanoma cancers in skin excisions, a short wavelength such as blue  $488 \text{ nm}$  from an argon-ion laser is preferable. The blue wavelength would provide increased back-scatter and improved signal, as well as thinner sectioning (because of shorter wavelength) in wider fields of view (lower NA and thus lower magnification may be used).

**Permanent histopathology is not affected by 5% acetic acid washing** The acetic acid does not create permanent changes in skin (Fig 4) that would alter the diagnostic information, if there is a

need to process the skin excisions for permanent paraffin-embedded histopathology. **Figure 4** does not show the compaction of chromatin that is clearly seen in **Fig 3**. (To observe the compaction of chromatin in **Fig 3**, the skin excisions were fixed in glutaraldehyde/paraformaldehyde, embedded in Epon plastic and stained with toluidine blue.) This is important because the diagnostic accuracy of routine permanent formalin-fixed, paraffin-embedded histology is not sacrificed. When preparing permanent sections, the intranuclear chromatin compaction is not retained during the tissue processing. Thus, the observed histology of the skin after washing with 5% acetic acid is equivalent to that without the acetic acid.

**Imaging in crossed polarization enhances the contrast for easy visualization of nonmelanoma cancer** The acetic acid-washed nuclei in the cancers significantly depolarize the linearly polarized illumination light (**Fig 5**). The compacted chromatin that fills up the intranuclear volume must cause multiple scattering of the linearly polarized illumination light. A confocal microscope detects singly back-scattered light, unless multiple scattering occurs within the small probe volume, as must happen due to the compacted chromatin. The multiple scattering must then cause depolarization, as is well known to occur in living tissues (MacKintosh *et al*, 1989; Schmitt *et al*, 1992; Demos *et al*, 1996; Demos and Alfano, 1997). The detected light from the surrounding cytoplasm and collagen is singly back-scattered, however, and therefore maintains its linear polarization. Cross-polarization is thus a simple but effective method to enhance the contrast of the cancer relative to the surrounding cytoplasm and dermis; we detect depolarized light from the nuclei but suppress the polarized light from the cytoplasm and collagen.

**Confocal examination of 1 mm thick skin excisions is similar to the procedure for examining histopathology sections** Normally, water immersion objective lenses of 0.7–1.2 NA are used that provide lateral resolution of 0.5–1.0  $\mu\text{m}$  and axial resolution (section thickness) of 2–5  $\mu\text{m}$  (Rajadhyaksha *et al*, 1995, 1999a,b). Such high NA are necessary for imaging nuclei and cells but we can only visualize small fields of view of typically 0.25–0.5 mm (e.g., **Figs 1a** and **2b**). Histopathology is, however, based on rapid examination of large fields of view of typically 8–2 mm with 2–8  $\times$  0.05–0.20 NA objective lenses. With objective lenses of such low NA, the Mohs surgeon first examines gross patterns of hematoxylin-stained (i.e., purple colored) nuclei within a background of eosin-stained (i.e., pink-colored) collagen; individual nuclei are not resolved. This is followed by high resolution inspection of the nuclei in suspected sites in small fields of view of typically 2–0.5 mm with 10–40  $\times$  0.25–0.65 NA objective lenses.

Low-resolution examination of large fields of view was achieved in the confocal microscope with objective lenses of lower NA and magnification. With 20 $\times$ –10 $\times$  0.3 NA water immersion lenses, the field of view increases to 1–2 mm whereas the axial resolution (section thickness) decreases to  $\approx$  30  $\mu\text{m}$  (experimentally measured). With this section thickness, individual nuclei are not resolved, but patterns of bright nuclei in larger fields can be visualized (**Figs 2a**, **5c**, and **6a**). Visualizing bright patterns of nuclei on a dark background of collagen is the confocal analog to histopathology in which purple (hematoxylin stained) patterns of nuclei are visualized on a pink (eosin stained) background of collagen.

Even the largest field of view (maximum 2 mm at present) with the confocal microscope is not adequate as the skin excisions are usually larger. Therefore, a mosaic or low-resolution map of the entire excision is created, showing the location and general morphology of the cancer (**Fig 8a**). With an automated stage translation and image digitizing routine, a mosaic of 10  $\times$  10 mm area of tissue can presently be created in 3.5 min. (Another system is being developed that will create mosaics of 20  $\times$  20 mm areas in 5 min.) Once a mosaic is rapidly made, the Mohs surgeon can quickly identify those fields that appear bright and are suspected to be cancerous; the nuclear morphology in the suspected fields is

then inspected at higher resolution. Fast confocal low-resolution examination of the entire excision, followed by careful high-resolution inspection of the nuclear morphology is thus similar to the examination of histopathology sections in Mohs micrographic surgery.

**Confounding features in confocal images are similar to those in histopathology sections** One confounding feature in Mohs histopathology sections is hair follicles as the nuclei in the follicular epithelium stain purple with hematoxylin, similar to the nuclei in cancer cells; at low resolution, normal follicles may mimic the gross morphology of cancer lobules. This can be particularly confounding when the cancer grows around a hair follicle, and necessitates examination of individual nuclei to distinguish cancerous cells reliably from normal hair follicle epithelium. The same situation presents itself using confocal microscopy. Hair follicles that appear in histology as purple-stained annular structures (*arrowheads* in **Fig 8b**) now appear in confocal images as annular bright structures (*arrowheads* in **Figs 5c** and **8a**). Again, changing from low resolution to high resolution is necessary to determine nuclear morphology. Furthermore, changing from crossed polarization to brightfield also helps in identifying hair follicles as well as sebaceous glands and fat cells. Changing focus also helps, to examine these structures in three dimensions. This, of course, is possible in real-time with the confocal microscope.

**Image understanding** As with any new imaging modality, understanding the images is the most critical factor for developing confocal reflectance microscopy into an accurate and repeatable method for noninvasive examination of nonmelanoma cancers in skin excisions during Mohs micrographic surgery; we must learn to interpret and analyze confocal images with sensitivity and specificity that competes with that of the gold standard (in this case, frozen histopathology). Further efforts are in progress to (i) perform clinical studies to correlate confocal mosaics (including the component high-resolution images) to histopathology, and (ii) improve the instrumentation, especially for image contrast, mosaicing speed, and tissue handling. A logical extension of this work is to develop confocal microscopy guided Mohs surgery: image BCC and SCC *in vivo*, to delineate cancer-to-normal tissue margins prior to surgery.

## SUMMARY

In summary, a simple method was developed to examine, with a confocal reflectance microscope, nonmelanoma cancers (BCC and SCC) in skin excisions during Mohs micrographic surgery without conventional (frozen) histopathology. We used 5% acetic acid and crossed polarization to enhance the contrast of the nuclei relative to the surrounding cytoplasm and dermis. Low-resolution confocal mosaics are rapidly made to examine large excisions and detect suspected cancerous fields, followed by high resolution inspection of the nuclear morphology in the suspected fields. This is similar to the procedure for examining histopathology. The preparation of noninvasive confocal sections is potentially possible within 5 min, instead of 20–45 min, which is currently required for frozen histopathology sections. At present, a mosaic of 10  $\times$  10 mm area of tissue can be created in 3.5 min; recent instrumentation developments have demonstrated the possibility of creating 20  $\times$  20 mm mosaics in 5 min. Further research must concentrate on improving our image understanding and our ability to read these images accurately. When that happens, both the patient and the Mohs surgeon will potentially save several hours per day in the operating room. Fast confocal reflectance microscopic examination of excisions may improve the management of surgical pathology and guide the microsurgery of any type of human tissue.

for their, as always, critical insights and advice. This work was funded by a grant from Lucid Inc. to Wellman Laboratories at Massachusetts General Hospital.

## REFERENCES

- Alberts B, Bray D, Lewis J, Raff M, Roberts K, Watson JD: *Molecular Biology of the Cell*, 2nd edn. New York: Garland Publishing Inc., 1989 pp 498–499
- Bertrand C, Corcuff P: In vivo spatio-temporal visualization of the human skin by real-time confocal microscopy. *Scanning* 16:150–154, 1994
- Brunsting A, Mullaney P: Differential light scattering from spherical mammalian cells. *Biophys J* 14:439–453, 1974
- Burghardt E: Über die atypische Umwandlungszone. *Geburtsh U Frauenheilk* 19:676, 1959
- Corcuff P, Leveque JL: In vivo vision of the human skin with the tandem scanning microscope. *Dermatology* 186:50–54, 1993
- Corcuff P, Bertrand C, Leveque JL: Morphometry of human epidermis in vivo by real-time confocal microscopy. *Arch Dermatol Res* 285:475–481, 1993
- Corcuff P, Gonnord G, Pierard GE, Leveque JL: In vivo confocal microscopy of human skin: a new design for cosmetology and dermatology. *Scanning* 18:351–355, 1996
- Demos SG, Alfano RR: Optical polarization imaging. *Appl Opt* 36:150–155, 1997
- Demos SG, Savage H, Heerdt AS, Schantz S, Alfano RR: Time-resolved degree of polarization for human breast tissue. *Opt Commun* 124:439–442, 1996
- Drezek RA, Collier T, Brookner CK, Malpica A, Lotan R, Richards-Kortum RR, Follen M: Laser scanning confocal microscopy of cervical tissue before and after application of acetic acid. *Am J Obstet Gynecol* 182:1135–1139, 2000
- Fawcett DW: *A Textbook of Histology*, 11th edn. Philadelphia: W.B. Saunders Co, 1986, pp 31–47
- Fraschini A, Pellicciari C, Biggiogera M, Romanini MGM: The effect of different fixatives on chromatin: cytochemical and ultrastructural approaches. *Histochem J* 13:763–779, 1981
- van de Hulst HC: *Light Scattering by Small Particles*. New York: Dover Publications, 1981
- Kaufman SC, Beuerman RW, Greer DL: Confocal microscopy: a new tool for the study of the nail unit. *J Am Acad Dermatol* 32:668–670, 1995
- MacKintosh FC, Zhu JX, Pine DJ, Weitz DA: Polarization memory of multiply scattered light. *Phys Rev B* 40:9342–9345, 1989
- Marwick C: New light on skin cancer mechanisms. *JAMA* 275:445–446, 1995
- Masters BR, Gonnord G, Corcuff P: Three-dimensional microscopic biopsy of in vivo human skin: a new technique based on a flexible confocal microscope. *J Microsc* 185: 329–338, 1997a
- Masters BR, Aziz DJ, Gmitro AF, Kerr JH, O'Grady TC, Goldman L: Rapid observation of unfixed, unstained human skin biopsy specimens with confocal microscopy and visualization. *J Biomed Opt* 2:437–445, 1997b
- Mikhail GR (ed.): *Mohs Micrographic Surgery*. Philadelphia: W.B. Saunders, 1991
- Mohs FE: Chemosurgery—a microscopically controlled method of cancer excision. *Arch Surg* 42:279–295, 1941
- New KC, Petroll WM, Boyde A, et al: In vivo imaging of human teeth and skin using real-time confocal microscopy. *Scanning* 13:369–372, 1991
- Rajadhyaksha M, Grossman M, Esterowitz D, Webb RH, Anderson RR: In vivo confocal scanning laser microscopy of human skin: melanin provides strong contrast. *J Invest Dermatol* 104:946–952, 1995
- Rajadhyaksha M, González S, Zavislan JM, Anderson RR, Webb RH: In vivo confocal scanning laser microscopy of human skin II. advances in instrumentation and comparison with histology. *J Invest Dermatol* 113:293–303, 1999a
- Rajadhyaksha M, Anderson RR, Webb RH: Video-rate confocal scanning laser microscope for imaging human tissues in vivo. *Appl Opt* 10:2105–2115, 1999b
- Schmitt JM, Gandjbakhche AH, Bonner RR: Use of polarized light to discriminate short-path photons in a multiply scattering medium. *Appl Opt* 31:6535–6546, 1992
- Smithpeter C, Dunn A, Drezek R, Collier T, Richards-Kortum R: Near real-time confocal microscopy of cultured amelanotic cells: sources of signal, contrast agents and limits of contrast. *J Biomed Opt* 3:429–436, 1998
- Tearney GJ, Brezinski ME, Southern JF, Bouma BE, Hee MR, Fujimoto JG: Determination of the refractive index of highly scattering human tissue by optical coherence tomography. *Opt Lett* 20:2258–2260, 1995